Analytica Chimica Acta 812 (2014) 33–40

Contents lists available at ScienceDirect

Analytica Chimica Acta

journal homepage: www.elsevier.com/locate/aca

Highly sensitive electrogenerated chemiluminescence biosensor in profiling protein kinase activity and inhibition using a multifunctional nanoprobe

Ru-Ping Liang, Cai-Yun Xiang, Hui-Fang Zhao, Jian-Ding Qiu*

Department of Chemistry, Nanchang University, Nanchang 330031, PR China

HIGHLIGHTS

- We reported a novel ECL biosensor for sensitive analysis of protein kinase activity.
- GOx/Au NPs/DNA-biotin was used as the ECL signal amplification nanoprobe.
- This strategy can in situ generate coreactant H_2O_2 to improve the luminol ECL signal.
- Highly sensitive detection of PKA activity and inhibition is achieved.

GRAPHICAL ABSTRACT

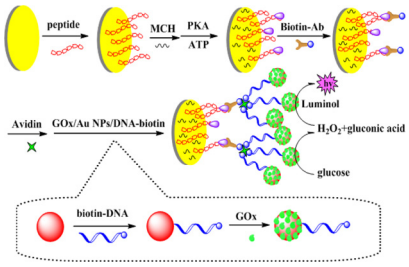

ARTICLE INFO

Article history:
Received 14 November 2013
Received in revised form
16 December 2013
Accepted 23 December 2013
Available online 3 January 2014

Keywords:
Electrogenerated chemiluminescence
Protein kinase A
Multifunctional nanoprobe
Ellagic acid

ABSTRACT

We presented a novel electrogenerated chemiluminescence (ECL) biosensor for monitoring the activity and inhibition of protein kinases based on signal amplification using enzyme-functionalized Au NPs nanoprobe. In this design, the biotin-DNA labeled glucose oxidase/Au NPs (GOx/Au NPs/DNA-biotin) nanoprobes, prepared by conjugating Au NPs with biotin-DNA and GOx, were bound to the biotinylated anti-phosphoserine labeled phosphorylated peptide modified electrode surface through a biotin–avidin interaction. The GOx assembled on the nanoprobe can catalyze glucose to generate H_2O_2 in the presence of O_2 while the ECL reaction occurred in the luminol ECL biosensor. At a higher concentration of kinase, there are more nanoprobes on the electrode, which gives a higher amount of GOx at the electrode interface and thus higher electrocatalytic efficiency to the luminol ECL reaction. Therefore, the activity of protein kinases can be monitored by ECL with high sensitivity. Protein kinase A (PKA), an important enzyme in regulation of glycogen, sugar, and lipid metabolism in the human body, was used as a model to confirm the present proof-of-concept strategy. The as-proposed biosensor presents high sensitivity, low detection limit of 0.013 U mL^{-1}, wide linear range (from 0.02 to 40 U mL^{-1}), and excellent stability. Moreover, this biosensor can also be used for quantitative analysis of kinase inhibition. On the basis of the inhibitor concentration dependent ECL signal, the half-maximal inhibition value IC_{50} of ellagic acid, a typical PKA inhibitor, was estimated, which is in agreement with those obtained using the conventional kinase assay. The simple and sensitive biosensor is promising in developing a high-through assay of in vitro kinase activity and inhibitor screening for clinic diagnostic and drug development.

1. Introduction

Protein phosphorylation, catalyzed by hundreds of different protein kinases, plays a key role in the regulation of signal transduction networks [1,2] and the modulation of many cellular functions such as cellular proliferation [3], hormone secretion [4],

* Corresponding author. Tel.: +86 791 83969518.
E-mail address: jdqiu@ncu.edu.cn (J.-D. Qiu).

0003-2670/$ – see front matter © 2013 Elsevier B.V. All rights reserved.
http://dx.doi.org/10.1016/j.aca.2013.12.037

gene transcription [5] and cell differentiation [6]. Protein kinases catalyze the transfer of a phosphate group from adenosine 5′-triphosphate (ATP) to the OH group of an amino acid side chain in peptides or proteins, accompanied by generating adenosine diphosphate (ADP) [7]. Most kinases act on serine and threonine; others act on tyrosine and a number of so-called dual-specificity kinases act on all of the three. Protein kinases regulate cellular processes by a highly controlled series of phosphorylation reactions, frequently with some kinases acting as substrates for other kinases [8]. The over-expression of protein kinases causes various diseases such as diabetes, aggressive tumor or Alzheimer's disease and chronic inflammatory disease [9–12]. As a result, the detection of phosphorylation and the assay of protein kinase activity and their potential inhibitors have become a critical topic, which is not only valuable to provide insights regarding the fundamental biochemical process of diseases but also essential to the protein kinase-targeted drug discovery and molecular-target therapies.

Up to now, traditional methods for the measurement of protein kinase activities include isotope labeling technique [13–16], fluorescence polarization [17,18], mass spectroscopy [19], and surface plasmon resonance (SPR) analysis system [20]. However, these methods were time-consuming, laborious, complex or costly. For overcoming the above limitations, many new detection strategies based on field-effect transistor (FET) devices [21], contact-angle measurements [22], electrochemistry [23], and electrochemiluminescence (ECL) sensing have been proposed. Among these methods, the ECL producing light by an oxidation or reduction reaction at an electrode surface has been proved to be a useful tool for kinase activity detection due to its high versatility, simplified optical setup, good temporal and spatial control, fast sample analysis, and a very low background signal [24,25]. However, only few ECL biosensors for protein kinases activity assay have been reported recently, which are potential systems for highly sensing but strongly neglected.

The rapid development of nanostructured materials promotes the evolution of high-performance ECL biosensors due to their unique chemical, physical properties and great analytical potential [26–28]. Au NPs come to the avant-courier and are widely applied in bioassay [29,30] due to their promising catalytic properties, large specific surface area, excellent conductivity, good biocompatibility, and highly catalytic activity to the ECL process of luminol in chemical reaction [31–33]. For example, Xu et al. used ultrahigh amplification efficiency of Au NPs to the luminol ECL reaction to develop a novel ECL biosensor for the kinase activity and inhibition analysis [34]. Zhao et al. utilized DNA-modified Au NPs which can absorb a great deal of tris(2,2′-bipyridyl)ruthenium(II)[Ru(II)] by electrostatic interaction to develop a novel ECL method for protein kinase activity and inhibition monitoring [35]. However, to the best of our knowledge, so far no Au NPs as either carriers of conventional active labels such as enzymes and electroactive species or catalysts have been employed for detecting activities of protein kinases and inhibition assay.

In this work, a novel ECL biosensor for sensitive analysis of the kinase activity and inhibition was proposed by using GOx/Au NPs/DNA-biotin as the ECL signal amplification probe. The GOx/Au NPs/DNA-biotin probe was prepared by sequentially immobilizing biotin-DNA and then GOx to Au NPs. When PKA is present in solution, the assembled peptides on gold electrode surface will be phosphorylated to form phosphoserine which is subsequently recognized by biotinylated anti-phosphoserine. Upon addition of GOx/Au NPs/DNA-biotin nanoprobe and avidin in this system, multiple nanoprobe can be immobilized on the biotinylated anti-phosphoserine modified electrode surface via avidin–biotin reaction. The assembled GOx catalyzes the oxidation of glucose in the presence of dissolved oxygen to form H_2O_2 in situ, which is coreactant for luminol ECL. In this concept, one phosphoserine group can capture large amount of GOx. When excess glucose is present in the system, large amount of H_2O_2 will be produced, forming considerably amplified ECL signal. In addition, Au NPs can also catalyze the ECL process of luminol in chemical reactions, further enhance the ECL signal. The proposed strategy not only shows the mimicking bi-enzyme synergetic catalysis of Au NPs and GOx to increase the ECL signal but also overcome the shortage of instability of H_2O_2 as coreactant by in situ generating H_2O_2 from the glucose catalyzed by GOx to enhance the sensitivity of ECL detection. Therefore, the present sensor can sensitively monitor the kinase activity and inhibition.

2. Experimental

2.1. Materials and reagents

Protein kinase A (PKA, catalytic subunit from recombinant *E. coli* strain) was obtained from New England Biolabs. Cysteine-terminated peptide (H-CGGGGLSARRL-OH) was purchased from GL Biochem Ltd. (Shanghai, China). Adenosine 5′-triphosphate (ATP) disodium salt, ellagic acid (4,4′,5,5′,6,6′-hexahydroxydiphenic acid 2,6,2′,6′-dilactone), biotinylated monoclonal anti-phosphoserine, mercaptohexanol (MCH), hydrogen tetrachloroaurate ($HAuCl_4{\cdot}4H_2O$), avidin, glucose oxidase (GOx), and luminol were purchased from Sigma–Aldrich. Biotin-DNA (5′-biotin-GAGTTGTCGGTGTAGGTCG-$(CH_2)_3$-SH-3′) was synthesized by Sangon Biotech Co., Ltd. (Shanghai, China). All other regents were of analytical grade and were used as received without further purification. All aqueous solutions were prepared and diluted with ultrapure and sterilized water.

2.2. Apparatus

The UV–vis absorption spectra were collected on a Shimadzu UV-2450 spectrophotometer. Atomic force microscopy (AFM) images were recorded under the mode of ScanAsyst using Bruker MultiMode-8 atomic force microscopy. Electrochemical measurements were carried out on an Autolab PGSTAT30 electrochemical workstation (Eco Chemie, Netherlands). The cyclic voltammograms were recorded in voltage sweeps between −0.1 and 0.6 V with a sweep rate of 100 mV s^{-1}. Electrochemical impedance spectroscopy measurements were performed by applying an ac voltage of 5 mV amplitude over a frequency range of 0.01–10^5 Hz. The ECL measurements were carried out on an MPI-B multifunctional electrochemical analytical system (Xi'an Remex Analytical Instrument Ltd. Co., China). The system provided an electrochemical potentiostat (0–2.5 V) for the ECL detection, a multifunction chemiluminescence detector and a multichannel data collection analyzer to connect with the other parts. Output ECL intensity was amplified and recorded in a computer using the MPI-B software. ECL intensities were measured through the bottom of the cell with a photomultiplier tube window and all of them were enclosed in a light-tight box. The ECL cell was composed of a modified gold working electrode (φ = 2 mm), an Ag/AgCl reference electrode (KCl saturated), and a Pt wire counter electrode.

2.3. Preparation of nanoprobe

The gold nanoparticles (Au NPs) were prepared as reported previously [36,37]. In brief, 50 mL of 0.05 g L^{-1} $HAuCl_4{\cdot}4H_2O$ solution was added into a 100 mL round flask, and was heated to boiling. Then, 5 mL of 1% sodium citrate solution was added rapidly under vigorous stirring. The solution was maintained at the boiling state for 10 min. The color changed from yellow to deep wine red, demonstrating the formation of a stable and monodispersed Au NPs colloidal solution which was stored at 4 °C prior to use.

A 0.3 mL (1 μM) of biotin-DNA was first added into 5 mL (14 nM) of Au NPs solution. After incubation for 24 h, the DNA-modified Au NPs solution was salt-stabilized with 0.1 M NaCl. Then, 0.2 mL of 2 mg mL^{-1} GOx was added to 0.2 mL of the upper solution. After incubation at 25 °C under gentle stirring for 1 h, 1 mL of 1% BSA solution was added to passivate the remaining active sites on Au NPs. The resulting solution was centrifuged at 13,000 rpm at 4 °C for 10 min, and the supernatant was removed. The final nanoprobe (GOx/Au NPs/DNA-biotin) was redispersed in 10 mM PBS (pH 7.4) containing 0.1 M NaCl and used immediately.

2.4. Assembly and phosphorylation of peptide on gold electrode

A gold electrode (diameter of 2 mm) was polished carefully with 1.0, 0.3, and 0.05 μm α-Al_2O_3 powder on a piece of polishing cloth and then thoroughly rinsed with ethanol and water. Prior to the immobilization of peptide, the gold electrode was scanned in 0.5 M H_2SO_4 between −0.2 and 1.55 V (vs Ag/AgCl) until a reproducible cyclic voltammogram was obtained. The cleaned gold electrode was then immersed into a 100 μM cysteine-terminated peptide solution at room temperature in darkness for 16 h. After thorough rinsing with blank PBS, the peptide modified electrode was immersed in a 5 mM MCH solution for 1 h to block the nonspecific binding sites on the gold electrode. When the peptide modified electrode was incubated into an assay buffer solution (20 mM Tris–HCl and 20 mM $MgCl_2$, pH 7.4) containing a desired amount of PKA and ATP at 30 °C for 1 h, a phosphate group can be transferred from ATP to the peptides, resulting in a phosphorylated peptide modified electrode. In the inhibition experiment, a desired concentration of inhibitor (0, 1, 3, 5, 7, 10, 15 and 30 μM) was also contained in the assay buffer solutions, and the procedures were similar as above.

2.5. ECL characterization and kinase activity detection

The phosphorylated peptide modified electrode was first immersed into the biotinylated anti-phosphoserine solution at 37 °C for 1 h. After thorough rinsing with blank PBS, 200 μL of 0.1 mg mL^{-1} avidin was added and incubated for 30 min at room temperature. The resulted avidin-labeled biotinylated anti-phosphoserine modified electrode was then incubated with 200 μL of GOx/Au NPs/DNA-biotin nanoprobe for 1 h at room temperature. After careful washing with blank PBS, the modified electrode was characterized by an ECL technique in a 100 μM luminol solution. In the protocol, H_2O_2, as the most widely used coreactant for luminol ECL, was generated in situ from the enzymatic reaction of glucose and dissolved oxygen catalyzed by GOx of the GOx/Au NPs/DNA-biotin nanoprobe. With increasing the concentration of PKA, more phosphate groups can be transferred from ATP to the peptide modified electrode, resulting in the increased density of GOx/Au NPs/DNA-biotin nanoprobe assembled onto the electrode surface, and thus a stronger ECL emission could be observed. This ECL intensity directly reflects the concentration of PKA and in turn the kinase activity can be detected sensitively.

3. Results and discussion

3.1. ECL strategy for kinase activity detection

The proposed ECL amplification strategy for the kinase activity analysis is illustrated in Scheme 1. Cysteine-terminated peptide is immobilized on a gold electrode through the Au—S bond to form a densely self-assembled monolayer and is further passivated by incubation with MCH. After phosphorylation reaction carried out in the presence of PKA using ATP as the cosubstrate, the phosphate groups are transferred to the serine residues of substrate peptide. The biotinylated anti-phosphoserine is then bound to the phosphoserine site due to the specific antibody-antigen interaction. Thus, multiple GOx/Au NPs/DNA-biotin nanoprobe fabricated by assembling biotin-DNA and GOx on Au NPs (inset in Scheme 1) can be effectively captured onto the biotin-labeled phosphorylated peptide modified electrode surface by using avidin as a bridge. Meanwhile, the existence of a long DNA strand on the GOx/Au NPs/DNA-biotin nanoprobe would obviate the steric effect and facilitate the assembling of numerous nanoprobes on the electrode surface. The introduced GOx can catalyze glucose to in situ generate H_2O_2 which is a coreactant of luminol ECL reaction, thus considerably amplifying the ECL signal. In addition, Au NPs can also catalyze the ECL process of luminol in chemical reactions, further enhance the ECL signal. Therefore, sensitive ECL detecting the phosphorylation and assaying PKA activity can be achieved.

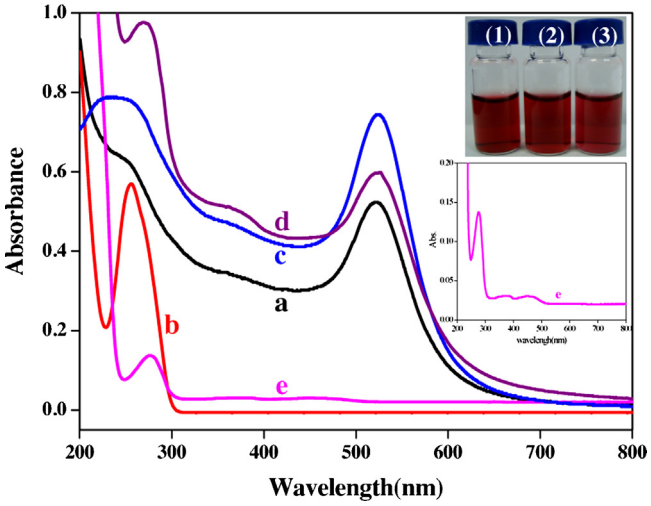

Fig. 1. UV–vis spectra of Au NPs (a), DNA (b), Au NPs/DNA-biotin (c), GOx/Au NPs/DNA-biotin (d), and GOx (e). Inset: the photographic pictures of Au NPs (bottle 1), Au NPs/DNA-biotin (bottle 2), and GOx/Au NPs/DNA-biotin (bottle 3).

3.2. UV–vis characterization of nanoprobe

UV–vis spectra were used to demonstrate the successful binding of the biotin-DNA strand and GOx to Au NPs (Fig. 1). The size of Au NPs is estimated to be ca. 14 nm from the absorption peak at 520 nm (curve a). After the biotin-DNA strand was attached on the surface of the Au NPs, an obvious absorption peak occurred at about 257 nm for DNA strand (curve b), and the Au NPs displayed a modest red-shift in the surface plasmon band from 520 nm to 525 nm (curve c), indicating the successful binding of biotin-DNA. After further capture of GOx onto the biotin-DNA labeled Au NPs surface, two characteristic absorption peaks located at 268 nm and 527 nm could be observed (curve d). Compared with Au NPs/DNA-biotin, the two absorption peaks exhibited a slight deviation, indicated an interaction between Au NPs and GOx occurred. Moreover, absorption peak at about 365 nm can be observed for the GOx/Au NPs/DNA-biotin nanoprobe (curve d), which is similar to the absorption of native GOx (curve e), indicating that GOx keeps its natural structure in these nanoprobes. The photos as inset in Fig. 1 shows that the Au NPs solution was homogeneous and deep reddish purple (bottle 1). After binding of the biotin-DNA strand (bottle 2) and GOx (bottle 3), no distinct color change or precipitates in the mixture of functionalized Au NPs was observed, indicating that the GOx/Au NPs/DNA-biotin nanoprobe has excellent stability even in 0.1 M NaCl solution.

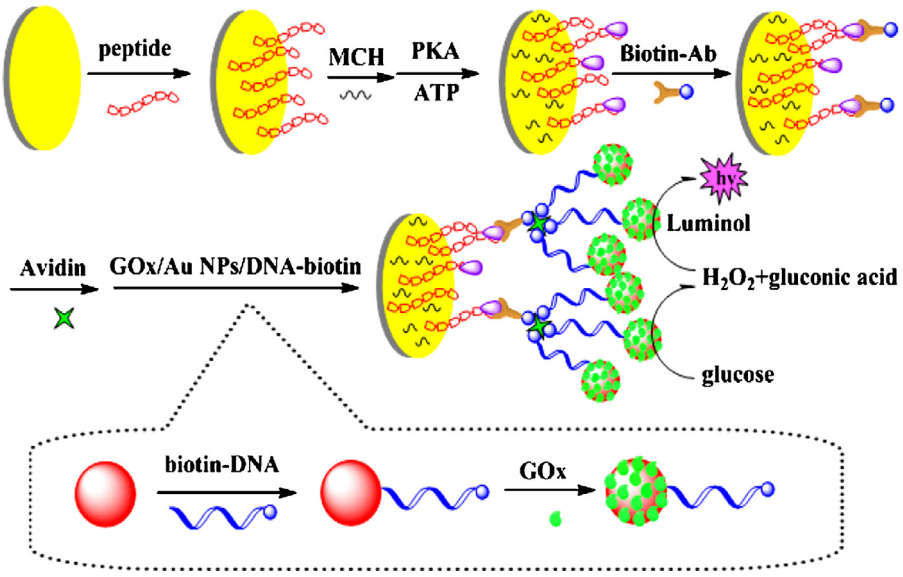

Scheme 1. Illustration of the ECL biosensor for monitoring PKA activity and inhibitor screening.

3.3. Characterization of the biosensors

The fabrication process of the ECL biosensor was first characterized by the atomic force microscopy (AFM) technique. Fig. 2A shows the image of peptide modified gold substrate. Plenty of hillocks with a height of ca. 3.0 nm suggested the successful assembly of peptides onto the electrode surface. After biotinylated anti-phosphoserine was bound to the phosphorylated peptide modified gold substrate surface, larger light dots were observed and the height increased to ca. 30 nm, and the aggregation of some biotinylated anti-phosphoserine molecules could be observed (Fig. 2B). When the GOx/Au NPs/DNA-biotin nanoprobe was further assembled on the electrode surface, the height increased to ca. 60 nm obviously (Fig. 2C). In addition, a number of island-like prominences appeared, which was clearly distinguished from Fig. 2B, confirming the assembly of GOx/Au NPs/DNA-biotin nanoprobe to the biotinylated anti-phosphoserine/phosphorylated peptide modified electrode surface.

The cyclic voltammetry (CV) was used to characterize the step-by-step buildup process of the modified electrode using $Fe(CN)_6^{3-/4-}$ as electroactive probe couple (Fig. 3). A couple of quasi-reversible redox peaks of the probe were obtained on the bare gold electrode (curve a). When the gold electrode was treated with cysteine-terminated peptide, the formed monolayer of peptide resulted in a decrease in the redox peak current (curve b). This decrease can be ascribed to the electron inert feature of the immobilized peptide partially blocking the electron transfer and mass transfer of $Fe(CN)_6^{3-/4-}$ ions to the gold electrode surface. After incubation of peptide modified electrode with PKA and ATP, a further decrease in current could be measured (curve c), indicating that phosphate groups had been transferred from ATP to peptide under the catalysis of PKA. After the consecutive assembling of biotinylated anti-phosphoserine, avidin, especially GOx/Au NPs/DNA-biotin nanoprobe on the phosphorylated peptide modified electrode surface, obvious current decrease of the anodic and cathodic peaks was observed (curves d–f). The phenomena demonstrated that the formed immunocomplexes on the electrode surface acted as inert electron and mass-transfer blocking layer which hindered the electron-transfer of $Fe(CN)_6^{3-/4-}$. The magnitude of the decrease in current is related to the activity of the PKA and the phosphorylation degree of the peptide molecules assembled on the electrode surface.

Electrochemical impedance spectroscopy (EIS) is an alternative powerful tool for monitoring the change of interfacial properties

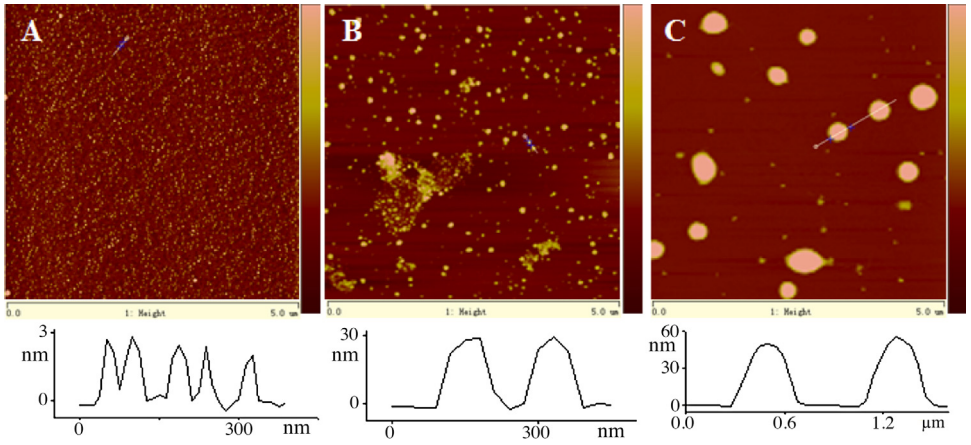

Fig. 2. AFM images of the cysteine-terminated peptide modified gold substrate (A), biotinylated anti-phosphoserine/phosphorylated peptide modified gold substrate before (B) and after (C) the assembly of GOx/Au NPs/DNA-biotin nanoprobe.

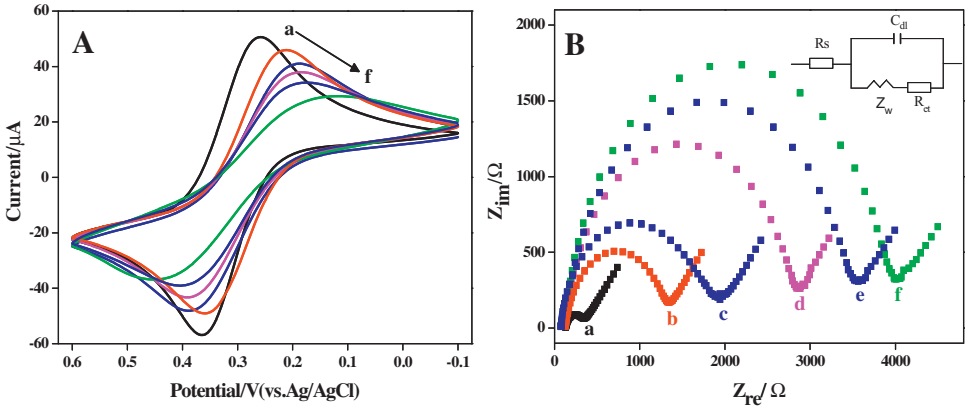

Fig. 3. Cyclic voltammograms (A) and electrochemical impedance spectra (B) of a bare gold electrode (a), a peptide modified gold electrode (b), a phosphorylated peptide modified electrode before (c) and after (d) the assembly of biotinylated anti-phosphoserine, then assembly of avidin (e) and GOx/Au NPs/DNA-biotin nanoprobe (f) in 5 mM $Fe(CN)_6^{3-/4-}$ solution containing 0.1 M KCl.

at electrode surfaces [38]. The EIS results of different modified electrodes in the presence of redox probe $Fe(CN)_6^{3-/4-}$ are shown in Fig. 3B. The bare electrode exhibited an almost straight line, the characteristics of a diffusional limiting step of the electrochemical process (curve a). After the electrode was treated with peptide, the electron-transfer resistance (R_{et}) remarkably increased to 1290 Ω (curve b), indicating the successful assembly of peptide on the electrode surface. The R_{et} increased further to 1955 Ω after PKA-catalyzed phosphorylation (curve c), and the R_{et} increased again after the consecutive assembling of biotinylated anti-phosphoserine, avidin, and GOx/Au NPs/DNA-biotin nanoprobe (curves d–f), which was consistent with the result of Fig. 3A. To give more detailed information about the impedance of the modified electrode, a modified Randle-sequivalent circuit (inset in Fig. 3B) was chosen to fit the measured results.

3.4. ECL behavior of the biosensor

Fig. 4 shows the ECL emission as a function of potential on the bare electrode, phosphorylated peptide modified electrode before and after treatment with GOx/Au NPs/DNA-biotin nanoprobe in 0.1 M pH 7.6 PBS solution containing 100 μM luminol and 10 mM glucose. It is clear that an ECL peak at about 0.55 V resulting from the ECL reaction of luminol was observed [39]. The bare gold electrode (curve a) and phosphorylated peptide modified electrode (curve b) exhibited much weaker ECL signal. However, when the GOx/Au NPs/DNA-biotin nanoprobe was assembled onto the phosphorylated peptide modified electrode surface, the ECL peak was enhanced obviously (curve c), which was nearly ten times larger than that of the phosphorylated peptide modified electrode. In the presence of GOx and glucose, the mechanism of the ECL reaction of luminol can be expressed as follows [34]:

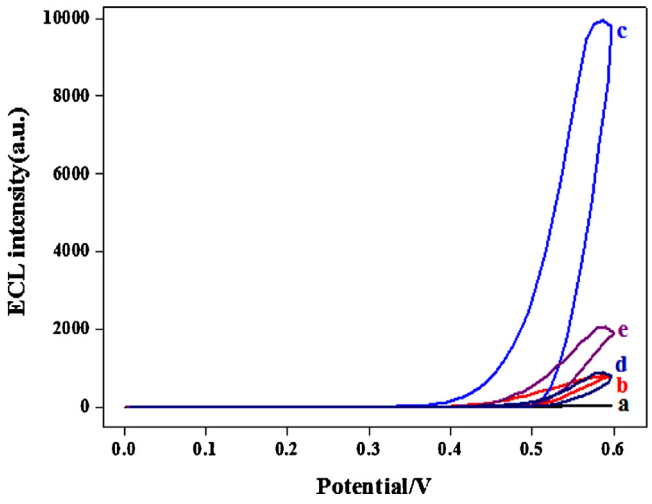

Fig. 4. ECL-potential curves of bare gold electrode (a), phosphorylated peptide modified electrode (b), electrode (b) after the treatment with GOx/Au NPs/DNA-biotin nanoprobe (c), Au NPs (d) and biotin-GOx (e) respectively. The assay was carried out in a Tris–HCl buffer solution (20 mM, pH 7.4) containing 20 mM $MgCl_2$, 50 μM ATP, and 50 U mL^{-1} PKA. The ECL measurements were performed in pH 7.6 PBS solution containing 100 μM luminol and 10 mM glucose at a scan rate of 100 mV s^{-1}.

$$\text{glucose} + O_2 \xrightarrow{\text{GOx}} \text{gluconic acid} + H_2O_2 \quad (1)$$

$$H_2O_2 \underset{+H^+}{\overset{-H^+}{\rightleftarrows}} HO_2^- \xrightarrow{-e} HO^\bullet{}_2 \underset{+H^+}{\overset{-H^+}{\rightleftarrows}} O^\bullet{}_2^- \quad (2)$$

$$LH^- - e^- \rightarrow LH^\bullet \rightarrow L^{\bullet -} + H^+ \quad (3)$$

$$L^{\bullet -} + O^\bullet{}_2^- \rightarrow LO_2^{2-} \quad (4)$$

$$LO_2^{2-} \rightarrow AP^{2-*} + N_2 \quad (5)$$

$$AP^{2-*} \rightarrow AP^{2-} + h\nu \quad (6)$$

where LH^- is the deprotonated luminol and AP^{2-*} is the excited state product. In this mechanism, H_2O_2 acts a coreactant to the ECL of luminol. Therefore, the concentration of H_2O_2 has a direct influence on the ECL signal of luminol. In this work, in situ generating H_2O_2 from the glucose catalyzed by GOx can increase the concentration of H_2O_2 near the surface of electrode [40], which significantly enhances the ECL intensity of luminol and thus greatly improves the sensitivity of the biosensor. In addition, Au NPs not only increase the loading capacity of the modified electrode to capture more GOx to amplify luminol ECL signals greatly but also catalyze the ECL process of luminol in chemical reactions. Thus, the Au NPs can mediate the ECL reaction even at a low content, implying highly efficient ECL signal amplification. At higher kinase activity, the more GOx/Au NPs/DNA-biotin nanoprobe could be effectively captured onto the phosphorylated peptide modified electrode surface. Thus, on one hand, larger numbers of Au NPs attached to the electrode surface could enhance the ECL intensity of luminol. On the other hand, a larger amount of GOx loaded on GOx/Au NPs/DNA-biotin nanoprobe could generate large amount of H_2O_2 in situ to increase the ECL intensity of luminol. On the basis of the enhanced ECL of luminol, kinase activity can be determined sensitively.

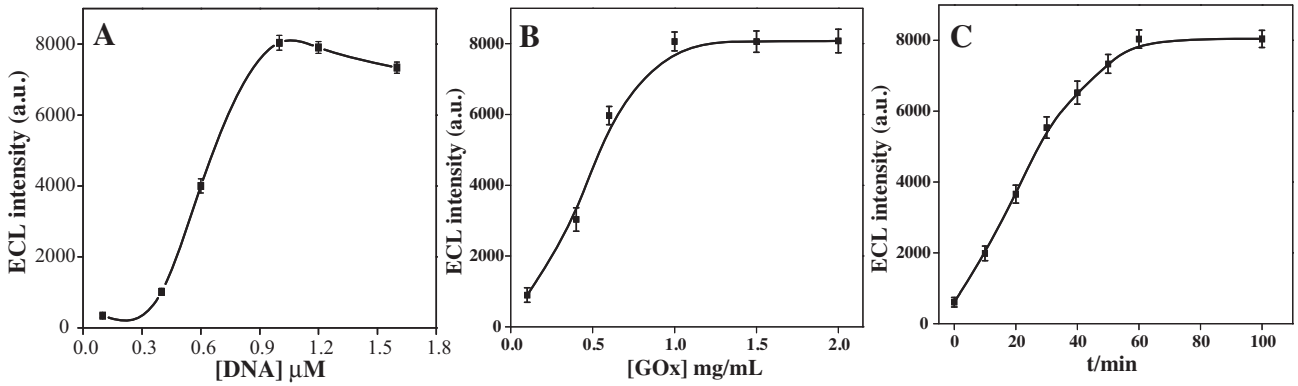

Fig. 5. Dependence of the ECL intensity on concentrations of biotin-DNA (A) and GOx (B) for preparation of nanoprobe, and the phosphorylation time (C). Other conditions are the same as those in Fig. 4.

To ensure the signal amplification ability of the GOx/Au NPs/DNA-biotin nanoprobe, control experiments were conducted. Results showed that the emission intensity of luminol after the assembly of GOx/Au NPs/DNA-biotin nanoprobe (curve c) was nearly ten times and five times larger than that of the phosphorylated peptide modified electrode treated with Au NPs (curve d) and biotin-GOx (curve e) respectively, indicating that the phosphorylation process as well as the PKA activity could be identified sensitively through the strategy. The present approach possesses several unprecedented advantages. First, the ECL biosensor offers a highly sensitive strategy based on the synergetic catalysis between Au NPs and GOx to amplify ECL signal of luminol. Secondly, this work utilizes the high surface-to-volume ratio of Au NPs to assemble a large amount of GOx to provide ECL signal amplification. Thirdly, in this luminol ECL biosensor, in situ generating H_2O_2 from the glucose catalyzed by GOx will overcome the shortage of instability of H_2O_2 as coreactant and improve the sensitivity and stability of the biosensor. Finally, avidin is a tetramer with four biotin binding sites arranged in two pairs on opposed faces of the molecule [41]. Thus, in this work, in addition to binding one biotinylated antiphosphoserine, a single avidin molecule could further bind three GOx/Au NPs/DNA-biotin nanoprobes to increase the amount of GOx and thus amplify the ECL signal. Accordingly, the as-proposed strategy provides a simple, sensitive, selective, and universal platform for kinase activity assay and inhibitor screening.

3.5. Optimization of conditions

The sensitivity of the proposed sensor is relied on the phosphorylation degree and the amount of the GOx/Au NPs/DNA-biotin nanoprobe captured on the electrode surface. The effect of the concentration of biotin-DNA and GOx for the construction of the nanoprobe and the effect of the reaction time of PKA catalyzing substrate peptides were investigated in the presence of PKA of 30 U mL^{-1}. As shown in Fig. 5A, the ECL intensity increased greatly as the concentration of biotin-DNA changed from 0.1 to 1.0 μM, followed by a decrease in the concentration range of 1.0–1.5 μM, which can be explained by the fact that the excessive biotin-DNA on the nanoprobe decreased the amount of GOx for signal amplification. Therefore, the optimal concentration of biotin-DNA was selected at 1.0 μM. As shown in Fig. 5B, with increasing GOx concentration from 0.1 to 1.0 mg mL^{-1} for the construction of the nanoprobe, the ECL intensity increased greatly. The further increase of GOx concentration did not obviously change the response, indicating that most of the surface sites on Au NPs were bound sufficiently. Thus, 1.0 mg mL^{-1} GOx was chosen as the optimal concentration for the preparation of the nanoprobe. The effect of reaction time of PKA catalyzing substrate peptides was also studied by stopping the catalyzing reaction at different time intervals and analyzing ECL signals output correspondingly. With increasing phosphorylation time, the ECL intensity showed an initial quick increase followed by a slow enhancement. No obvious change of the ECL intensity could be observed when the reaction was performed after 1 h (Fig. 5C). From these results, we gave the conclusion that 1 h was the optimal phosphorylation time and hence applied in the subsequent experiments.

3.6. ECL measurement of PKA activity

On the basis of the optimal conditions, the quantitative behavior of the proposed ECL method for the determination of PKA was assessed. Fig. 6A shows the ECL intensity versus time profiles with different concentrations of PKA. When the PKA units increased, the ECL signal increased accordingly and reached a saturation value once the concentration of PKA was above 80 U mL^{-1}. The increased ECL intensity was linearly proportional to the logarithm of the PKA concentration in the range from 0.02 to 40 U mL^{-1} (inset in Fig. 6A), which was much wider than those of previously reported 0.07–35 U mL^{-1} based on gold nanoparticles as signal transduction probes for the detection of kinase activity [34] and 0–1 U mL^{-1} based on specific binding of the phosphate groups with TiO_2 nanoparticles and multi-nanoparticle deposition through a signal transforming medium for profiling kinase activity [42]. The detection limit of PKA was 0.013 U mL^{-1} (signal-to-noise ratio of 3) which is much lower than those of 0.15 U mL^{-1} on a label-free electrochemical sensing strategy for profiling PKA activity based on Zr^{4+} mediated signal transition [23] and 0.45 U mL^{-1} on label-free fluorescent detection for monitoring the activity of PKA based on the aggregation behavior of unmodified CdTe quantum dots [43]. To further illustrate the good sensitivity of this assay, a control ECL measurement for the determination of PKA employing biotin-GOx instead of GOx/Au NPs/DNA-biotin nanoprobe was performed (Fig. 6B). The increased ECL intensity was linearly proportional to the logarithm of the PKA concentration in the range from 0.5 to 30 U mL^{-1}. The limit of detection is 0.1 U mL^{-1}, which is 7.7-fold higher than that of the GOx/Au NPs/DNA-biotin nanoprobe. Results indicate that employing the Au NPs as amplification carriers is an effective strategy.

Operational stability is one of the major concerns for practical application of a sensor. Fig. 7 displays the ECL emission of the biosensor under 25 cycles of continuous potential scans between 0 and 0.6 V (vs Ag/AgCl) in 0.1 M PBS containing 100 μM luminol and 10 mM glucose at 100 mV s^{-1}. Strong and stable ECL signals were observed with a relative standard deviation of 0.67%, which signified that the ECL biosensor possessed excellent potential cycling stability. The reproducibility of the ECL biosensor was also

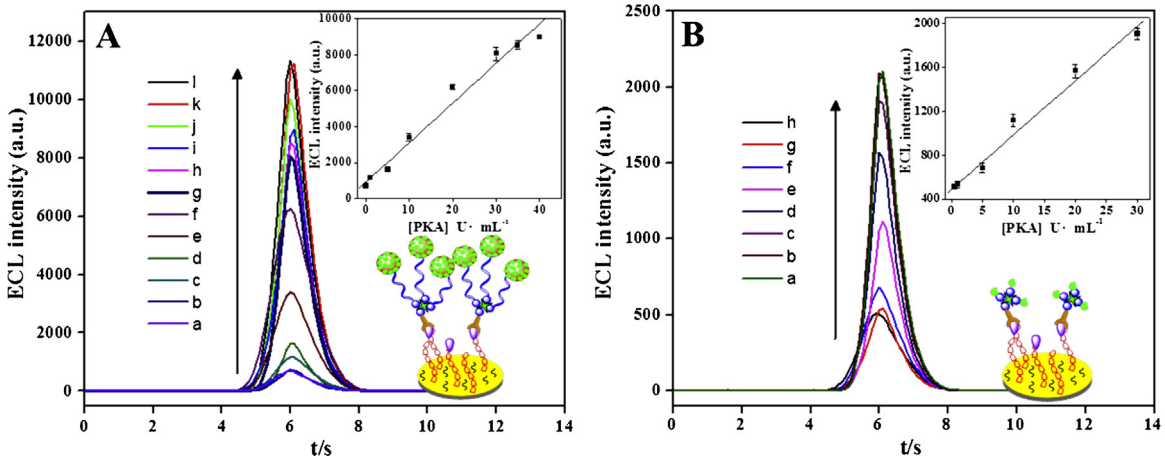

Fig. 6. ECL intensity–time profiles and the calibration curve of PKA in pH 7.6 PBS solution containing 100 μM luminol and 10 mM glucose. (A) ECL method in the presence of the GOx/Au NPs/DNA-biotin nanoprobe and different concentrations of PKA: 0.02 (a), 0.05 (b), 1 (c), 5 (d), 10 (e), 20 (f), 30 (g), 35 (h), 40 (i), 50 (j), 80 (k), and 100 U mL^{-1} (l). Inset: Calibration curve. (B) ECL method in the presence of biotin-GOx and different concentrations of PKA: 0.5 (a), 1 (b), 5 (c), 10 (d), 20 (e), 30 (f), 50 (g), and 100 U mL^{-1} (h). Other conditions are the same as those in Fig. 4.

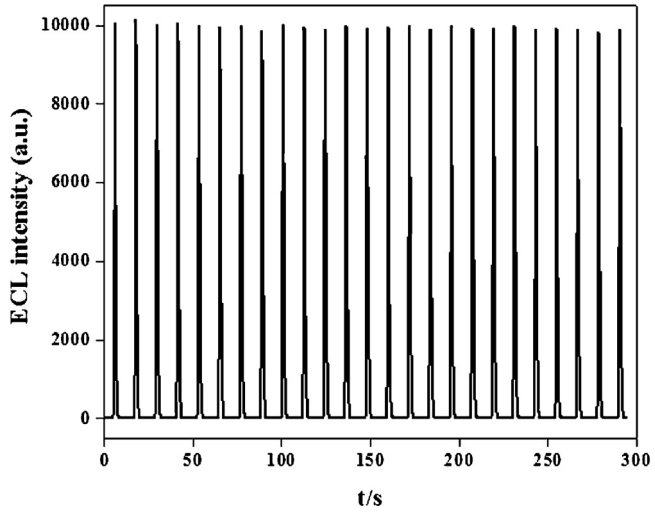

Fig. 7. ECL–time curves of the biosensor at PKA concentration of 50 U mL^{-1} under continuous cyclic voltammetry scan with a scan rate of 100 mV s^{-1}. Other conditions are the same as those in Fig. 4.

studied with intra- and inter-assay precision. The intra-assay precision of the ECL biosensor was evaluated by measuring 50 U mL^{-1} of PKA activity ten times. The inter-assay precision was assessed by assaying the same level of PKA activity with ten electrodes. The intra- and the inter-assay variation coefficients were 5.3% and 6.2%, respectively, demonstrating good performance of the designed strategy for the detection of PKA activity.

3.7. Kinase activity inhibition evaluation

The proposed method for the detection of phosphorylation was further employed to quantitatively characterize the inhibition of PKA activity. Herein, ellagic acid, possessing anti-mutagenic, and anti-carcinogenic properties as a potent and cell-permeable antioxidant [44], was employed for the model inhibitor in this research. As shown in Fig. 8A, the ECL signal decreased with the increasing concentration of ellagic acid. Only weak ECL signal was observed with the addition of ellagic acid at 10 μM. The inhibition of PKA activity on peptide using ellagic acid was monitored and an IC_{50} (inhibitor concentration producing 50% inhibition) was measured to be about 4.07 μM from curve a in Fig. 8B, which is in agreement with that reported in the literature obtained with conventional kinase assays [42,44]. In addition, DRB (5,6-dichlorobenzimidazole-1-β-D- ribofuranoside) and quercetin, tyrosine kinase inhibitor but not PKA

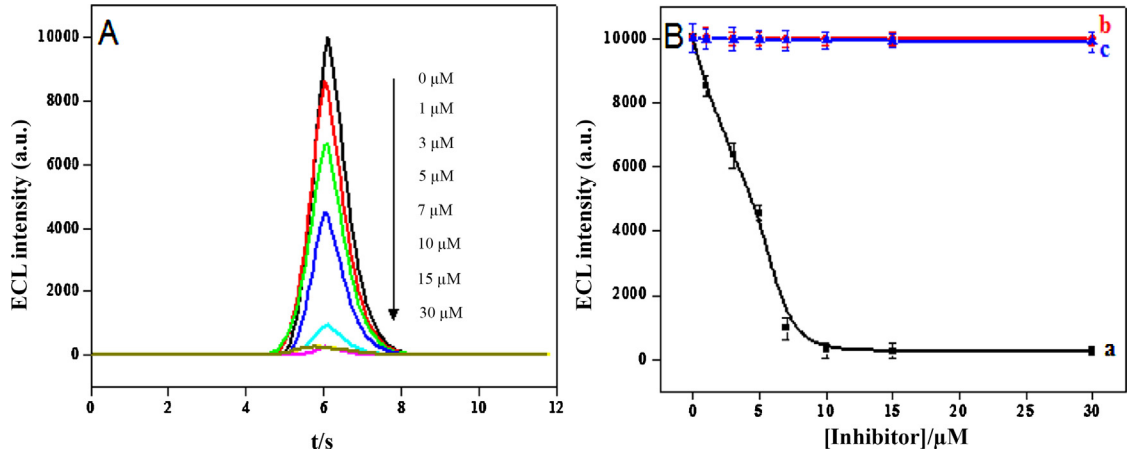

Fig. 8. (A) ECL intensity–time behaviors at different concentrations of ellagic acid. (B) The ECL intensity as a function of concentrations of ellagic acid (a), DRB (b), and quercetin (c). The phosphorylation of peptide was carried out with 50 U mL^{-1} PKA and 50 μM ATP. Other conditions are the same as those in Fig. 4.

inhibitor, were also added to evaluate the specificity of the fabricated ECL biosensor. As shown in curve b and curve c of Fig. 8B, the ECL signal had almost no change in the presence of these tyrosine kinase inhibitors with a concentration as high as 30 μM, showing an excellent specificity of the biosensor to kinase inhibitor profiling. These results indicated that the proposed GOx/Au NPs/DNA-biotin nanoprobe mediated ECL strategy is highly effective for quantitatively screening the activity of the kinase inhibitors.

4. Conclusion

In conclusion, a highly sensitive ECL sensing platform for the PKA analysis and inhibition screening has been fabricated using multifunctional nanoprobe as a signal transduction probe, by virtue of the synergetic catalysis between Au NPs and GOx and the high loading amount of GOx to amplify ECL signal of luminol. This strategy can in situ generate coreactant H_2O_2 to improve the luminol ECL signal during the measurements. As a result, the as-proposed ECL biosensor offers a highly sensitive strategy for PKA activity monitoring with a low detection limit of 0.013 U mL^{-1}, wide linear range, and good stability. Moreover, verified by using well-known kinase inhibition systems, the established sensor also shows excellent performance on the accurate and quantitative kinase inhibitor assay. The general and robust method can also be ready for other kinase activities and inhibition assays. Given the important roles of kinases in some disease related biological processes, this biosensor shows great potential for a high throughput assay in clinic diagnostics and drug discovery applications.

Acknowledgements

This work was supported by National Natural Science Foundation of China (21163014, 21105044 and 21265017), the Program for New Century Excellent Talents in University (NCET-11-1002).

References

[1] G. Manning, D.B. Whyte, R. Martinez, T. Hunter, S. Sudarsanam, Science 298 (2002) 1912–1934.
[2] S.S. Taylor, D.R. Knighton, J.H. Zheng, L.F. Teneyck, J.M. Sowadski, Annu. Rev. Cell. Biol. 8 (1992) 429–462.
[3] P.P. Roger, D. Christophe, J.E. Dumont, I. Pirson, Eur. J. Endocrinol. 137 (1997) 579–598.
[4] R.H. McCusker, D.R.J. Clemmons, Cell. Physiol. 174 (1998) 293–300.
[5] M. Montminy, Annu. Rev. Biochem. 66 (1997) 807–822.
[6] C. Bertolotto, P. Abbe, T.J. Hemesath, K. Bille, D.E. Fisher, J.P. Ortonne, R.J. Ballotti, Cell. Biol. 142 (1998) 827–835.
[7] M.E. Noble, J.A. Endicott, L.N. Johnson, Science 303 (2004) 1800–1805.
[8] E. Fayard, L.A. Tintignac, A. Baudry, B.A. Hemmings, Science 118 (2005) 5675–5678.
[9] I. Melnikova, J. Golden Nat. Rev. Drug Discov. 3 (2004) 993–994.
[10] R.I. Nicholson, J.M.W. Gee, M.E. Harper, Eur. J. Cancer 37 (2001) S9–S15.
[11] M. Sibilia, A. Fleischmann, A. Behrens, L. Stingl, J. Carroll, F.M. Watt, J. Schlessinger, E.F. Wagner, Cell 102 (2000) 211–220.
[12] D.P. Hanger, H.L. Byers, S. Wray, K.Y. Leung, M.J. Saxton, A. Seereeram, C.H. Reynolds, M.A. Ward, B.H. Anderton, J. Biol. Chem. 282 (2007) 23645–23654.
[13] P. Vandergeer, T. Hunter, Electrophoresis 15 (1994) 544–554.
[14] R.B. Pearson, B.E. Kemp, Method Enzymol. 200 (1991) 62–81.
[15] B.T. Houseman, J.H. Huh, S.J. Kron, M. Mrksich, Nat. Biotechnol. 20 (2002) 270–274.
[16] S.H. Diks, K. Kok, T. O'Toole, D.W. Hommes, P. Van Dijken, J. Joore, M.P. Peppelenbosch, J. Biol. Chem. 279 (2004) 49206–49213.
[17] H.W. Rhee, S.H. Lee, I.S. Shin, S.J. Choi, H.H. Park, K. Han, T.H. Park, J.I. Hong, Angew. Chem. Int. Ed. 49 (2010) 4919–4923.
[18] R.S. Agnes, F. Jernigan, J.R. Shell, V. Sharma, D.S. Lawrence, J. Am. Chem. Soc. 132 (2010) 6075–6080.
[19] S.A. Beausoleil, J. Villen, S.A. Gerber, J. Rush, S.P. Gygi, Nat. Biotechnol. 24 (2006) 1285–1292.
[20] P. Stenlund, A. Frostell-Karlsson, O.P. Karlsson, Anal. Biochem. 353 (2006) 217–225.
[21] R. Freeman, R. Gill, I. Willner, Chem. Commun. (2007) 3450–3452.
[22] A. Wieckowska, D. Li, R. Gill, I. Willner, Chem. Commun. (2008) 2376–2378.
[23] X. Xu, Z. Nie, J. Chen, Y. Fu, W. Li, Q. Shen, S. Yao, Chem. Commun. (2009) 6946–6948.
[24] M.M. Richter, Chem. Rev. 104 (2004) 3003–3036.
[25] P. Bertoncello, R.J. Forster, Biosens. Bioelectron. 24 (2009) 3191–3200.
[26] Y.Q. Yu, Q. Cao, M. Zhou, H. Cui, Biosens. Bioelectron. 43 (2013) 137–142.
[27] W.Y. Liu, Y. Zhang, S.G. Ge, X.R. Song, J.D. Huang, M. Yan, J.H. Yu, Anal. Chem. Acta 770 (2013) 132–139.
[28] F. Li, Y.Q. Yu, H. Cui, D. Yang, Z.P. Bian, Analyst 138 (2013) 1844–1850.
[29] J. Oishi, Y. Asami, T. Mori, J.H. Kang, M. Tanabe, T. Niidome, Y. Katayama, ChemBioChem 8 (2007) 875–879.
[30] T. Sawada, N. Shirakawa, Y. Hirai, M. Hashizume, M. Aizawa, T. Serizawa, Chem. Lett. 40 (2011) 142–143.
[31] R.J. Cui, H.C. Pan, J.J. Zhu, H.Y. Chen, Anal. Chem. 79 (2007) 8494–8501.
[32] G.F. Jie, P. Liu, S.S. Zhang, Chem. Commun. 46 (2010) 1323–1325.
[33] K.P. Liu, J.J. Zhang, C.M. Wang, J.J. Zhu, Biosens. Bioelectron. 26 (2011) 3627–3632.
[34] S.J. Xu, Y. Liu, T.H. Wang, J.H. Li, Anal. Chem. 82 (2010) 9566–9572.
[35] Z. Zhao, X. Zhou, D. Xing, Biosens. Bioelectron. 31 (2012) 299–304.
[36] K.C. Grabar, R.G. Freeman, M.B. Hommer, M.J. Natan, Anal. Chem. 67 (1995) 735–743.
[37] R.P. Liang, Z.X. Wang, L. Zhang, J.D. Qiu, Chem-Eur. J. 19 (2013) 5029–5033.
[38] S.M. Park, J.S. Yoo, Anal. Chem. 75 (2003) 455 A–461 A.
[39] H. Cui, Y. Xu, Z.F. Zhang, Anal. Chem. 76 (2004) 4002–4010.
[40] Y.L. Cao, R. Yuan, Y.Q. Chai, L. Mao, H. Niu, H.J. Liu, Y. Zhuo, Biosens. Bioelectron. 31 (2012) 305–309.
[41] M. Salmain, N. Fischer-Durand, L. Cavalier, B. Rudolf, J. Zakrzewski, G. Jaouen, Bioconjugate Chem. 13 (2002) 693–698.
[42] J. Ji, H. Yang, Y. Liu, H. Chen, J.L. Kong, B.H. Liu, Chem. Commun. (2009) 1508–1510.
[43] X.H. Xu, X. Liu, Z. Nie, Y.H. Pan, M.L. Guo, S.Z. Yao, Anal. Chem. 83 (2011) 52–59.
[44] G. Cozza, P. Bonvini, E. Zorzi, G. Poletto, M.A. Pagano, S. Sarno, A. Donella-Deana, G. Zagotto, A. Rosolen, L.A. Pinna, F. Meggio, S. Moro, J. Med. Chem. 49 (2006) 2363–2366.